

Article

Ex Situ Catalytic Pyrolysis of Invasive *Pennisetum purpureum* Grass with Activated Carbon for Upgrading Bio-Oil

Md Sumon Reza ^{1,2,3,*}, Shammya Afroze ⁴, Kairat Kuterbekov ⁴, Asset Kabyshev ⁴,
Kenzhebatyr Zh. Bekmyrza ⁴, Juntakan Taweekun ², Fairuzeta Ja'afar ⁵, Muhammad Saifullah Abu Bakar ³,
Abul K. Azad ³, Hridoy Roy ⁶ and Md. Shahinoor Islam ^{6,7,*}

- ¹ Faculty of Natural Sciences, L.N. Gumilyov Eurasian National University, Astana 010008, Kazakhstan
² Department of Mechanical and Mechatronics Engineering, Faculty of Engineering, Prince of Songkla University, Hatyai 90112, Thailand
³ Faculty of Integrated Technologies, Universiti Brunei Darussalam, Jalan Tungku Link, Gadong BE1410, Brunei
⁴ Faculty of Physics and Technical Sciences, L.N. Gumilyov Eurasian National University, Astana 010008, Kazakhstan
⁵ Chemical Sciences Programme, Faculty of Science, Universiti Brunei Darussalam, Jalan Tungku Link, Gadong BE1410, Brunei
⁶ Department of Chemical Engineering, Bangladesh University of Engineering and Technology, Dhaka 1000, Bangladesh
⁷ Department of Textile Engineering, Daffodil International University, Dhaka 1341, Bangladesh
* Correspondence: sumonce@gmail.com (M.S.R.); shahinoorislam@che.buet.ac.bd (M.S.I.)

Abstract: Energy demands keep increasing in this modern world as the world population increases, which leads to a reduction in fossil fuels. To resolve these challenges, *Pennisetum purpureum*, an invasive grass in Brunei Darussalam, was examined as the feedstock for renewable energy through a catalytic pyrolysis process. The activated carbon was applied as the catalyst for a simple and economical solution. The catalytic pyrolysis was executed at 500 °C (the temperature for the highest biofuel yield) for both reactors to produce the highest amount of upgraded biofuels. The biochar produced from the non-catalytic and catalytic pyrolysis processes showed a consistent yield due to stable operating conditions, from which the activated carbon was generated and used as the catalyst in this work. A significant amount of improvement was found in the production of biofuels, especially bio-oil. It was found that for catalysts, the number of phenolic, alcohol, furans, and ketones was increased by reducing the amount of acidic, aldehyde, miscellaneous oxygenated, and nitrogenous composites in bio-oils. The highest amount of phenolic compounds was produced due to a number of functional groups (-C=O and -OH) in activated carbon. The regenerated activated carbons also showed promising outcomes as catalysts for upgrading the bio-oils. The overall performance of synthesized and regenerated activated carbon as a catalyst in catalytic pyrolysis was highly promising for improving the quality and stability of bio-oil.

Keywords: invasive biomass; *Pennisetum purpureum*; catalytic pyrolysis; activated carbon; bio-oil; bioenergy



check for updates

Citation: Reza, M.S.; Afroze, S.; Kuterbekov, K.; Kabyshev, A.; Zh. Bekmyrza, K.; Taweekun, J.; Ja'afar, F.; Saifullah Abu Bakar, M.; Azad, A.K.; Roy, H.; et al. Ex Situ Catalytic Pyrolysis of Invasive *Pennisetum purpureum* Grass with Activated Carbon for Upgrading Bio-Oil. *Sustainability* **2023**, *15*, 7628. <https://doi.org/10.3390/su15097628>

Academic Editors: Kawnish Kirtania and Chayan K. Saha

Received: 7 March 2023

Revised: 1 May 2023

Accepted: 4 May 2023

Published: 6 May 2023



Copyright: © 2023 by the authors. Licensee MDPI, Basel, Switzerland. This article is an open access article distributed under the terms and conditions of the Creative Commons Attribution (CC BY) license (<https://creativecommons.org/licenses/by/4.0/>).

1. Introduction

Energy is among the most vital resources for the social and economic growth of any country; hence, the demand for energy is increasing daily. The primary source of energy is fossil fuel, which is depleting with time and produces greenhouse gases, particularly carbon dioxide (CO₂), during combustion [1–3]. As an alternative to fossil fuels, renewable energy sources are now highly attractive for researchers due to the effects of global climate change and environmental commitments. Renewable energy sources are mostly ecologically and economically friendly enough to be the replacement for the depletion of fossil fuel supplies. Biomass, wind, solar, geothermal, and tidal are the major renewable energy sources, where biomass to bioenergy is highly promising [4,5].

Among the biomass sources (municipal garbage, agricultural wastes, food waste, wood waste, grasses, etc.), invasive plants are the most important problems for biodiversity and have a negative effect on the ecosystem [6]. Only in North America are approximately 42% of the original species threatened by invasive species that cause environmental damages worth nearly USD 120 billion annually [7]. The most effective ways to utilize these invasive plants is in bioenergy technology as a sustainable energy source [8].

To produce bioenergy from invasive grasses, pyrolysis is the most practical process since it offers several benefits regarding storage, transportation, and solicitation flexibility [9]. In this process, biomass is converted into three main products: biochar, bio-oil, and syngas. Biochar is used to synthesize activated carbon (AC), improve soil quality, capture CO₂, and generate heat [10]. The bio-oils and syngas need to be purified before being used as fuel [11,12]. Bio-oils, produced by pyrolysis, generally contain volatile acids, water, and oxygenated compounds, which reduce the heating value of the oil [13]. Using catalysts, in the pyrolysis process, oxygenated and nitrogenous compounds can be reduced by enhancing the calorific value and stability of the bio-oils [14–16].

The most frequently used catalysts in the pyrolysis procedure are zeolites, metal oxides, natural catalysts, etc., which have some limitations, such as deactivation by blockage, the impossibility of using microporosity, and the generation of boehmite [17]. The utilization of activated carbon as a catalyst in the catalytic pyrolysis process can be a favorable solution because of its huge surface area, significant porosity, and strong structural strength. Recently, AC has shown exceptional catalytic performance in improving the quality of the chemicals in bio-oils [18]. In mixed catalysts, the hydrophobic nature of AC can prevent the deactivation of metal catalysts by water [19]. Very little research was performed on the synthesized AC as a catalyst in the catalytic pyrolysis process to figure out an economical and effective catalyst [20].

Pennisetum purpureum (also known as Elephant grass, Napier grass, or Uganda grass) is a C4 invasive perennial grass that can grow all over the world with a potential yield of 50–60 metric tons per hectare per six months [21]. The weed risk assessment score of the grass is very high, and it is a great threat to the ecosystem to dispose of it in landfills because it produces greenhouse gases [8]. In the tropical world, these grasses exhibit good biofuel production traits [22]. This invasive grass is highly available in Brunei Darussalam, and the product range is 5 tons/ha/yr. in dry circumstances and 55 tons/ha/yr in wet conditions [23]. Very little research has been conducted on bioenergy production from the invasive *P. purpureum* grass existing in Brunei Darussalam. The main objective of this work is to evaluate the upgradation of the bio-oil of invasive *P. purpureum* grass produced from the non-catalytic and catalytic pyrolysis processes by comparing the components of the bio-oils. The activated carbon produced from the same grass and the regenerated activated carbon were used as catalysts in this catalytic process to get an effective and economical solution.

2. Experimental

2.1. Biomass Sample Preparation

The *P. purpureum* grass was collected from the field of the Universiti Brunei Darussalam (UBD) and kept in direct sunlight for a week after cleaning and removing the debris. After that, the grass samples were placed in an oven for six hours at 100 °C to remove the moisture properly. Then, the samples were cut into small pieces and ground into small particles. Finally, the grass particles were sieved with the US standard sieve no. 60 (Sieve opening 250 µm) to achieve uniform samples smaller than 0.25 mm and packed in airtight bags. The biomass sample preparation diagram is explained in Figure S1.

2.2. Preparation of Activated Carbon (Catalyst)

The activated carbon was prepared from the biochar of *P. purpureum* grass through physicochemical activation processes. The biochar, produced at a 600 °C pyrolysis temperature, was used to prepare the activated carbon, as the higher temperature possesses

higher porosity with lower tars [24]. The biochar was mixed with potassium hydroxide (Assay $\geq 85.0\%$, made in Merck KGaA, Darmstadt, Germany) and water with a mass ratio of 1:4:5 (Biochar:KOH:Water) and kept in a beaker for 48 h [25]. After that, the mixture was oven-dried overnight at 100 °C temperature. Then, the dried mixture was pyrolyzed at 800 °C temperature for 1 h with a heating rate of 25 °C/min and nitrogen gas (99.99% purity) flow of 0.5 L/min. After pyrolysis, the activated carbon was washed with hot and acidic water to remove excess KOH to obtain neutral AC. Finally, the AC was dried in the oven and stored in a zipper bag. The size of the activated carbon was less than 0.25 mm due to the biomass sample size. The process of making activated carbon is shown in Figure S2.

2.3. Characterization of the Activated Carbon (SEM, BET, FTIR)

The surface morphology of the activated carbon was investigated at the Universiti Brunei Darussalam by a field emission scanning electron microscope (SEM) of the JSM-7610F Schottky, manufactured by JEOL, Akishima, Japan. The SEM images were captured at 25, 100, 1000, and 5000 magnifications without carbon coating to get the real pictures. The surface area of the activated carbon was evaluated using the Brunauer–Emmett–Teller (BET) method [26] with an ASAP2460, Micromeritics, USA, using nitrogen (N_2) adsorption at the Prince of Songkla University (PSU), Hat Tai, Thailand. The chemical groups of activated carbon were investigated at PSU using a Fourier-transform infrared (FTIR) spectrometer manufactured by Vertex 70, Bruker, Germany. The spectra were achieved for wavenumbers ranging from 4000 to 500 cm^{-1} with a 2 cm^{-1} phase size.

2.4. Regeneration of Activated Carbon (Catalyst)

The steam regeneration method was applied to regenerate the activated carbon. Initially, the activated carbon was washed with hot water to remove the major impurities [27]. Then, it was filtered and washed with acetone to remove the oil particles. The process was repeated several times back and forth as a method to get clean activated carbon. Finally, the activated carbon was washed with distilled water and dried in the oven at 100 °C for 6 h. The first-time regenerated and the second-time regenerated activated carbon were described as RAC-1 and RAC-2, respectively.

2.5. Biomass to Catalyst Ratio

The catalyst, used for this research was activated carbon prepared from the physio-chemical activation of the same source (*P. purpureum*). For all experiments, the biomass to catalyst ratio was maintained at 25:1 (wt.:wt.) to get an economical and realistic solution. Some of the researchers use a higher amount of catalyst than biomass to get the maximum effect of catalysts, which is uneconomical. For 1 g of catalyst, the mixture ratios of the catalysts are described in Table 1.

Table 1. List of catalysts and the biomass to catalyst ratios.

Catalyst Name	Catalyst Code	Biomass (wt.):Catalyst (wt.)
No catalyst	–	25 (g):0 (g)
Activated Carbon	AC	25 (g):1 (g)
First-Time Regenerated Activated Carbon	RAC-1	25 (g):1 (g)
Second-Time Regenerated Activated Carbon	RAC-2	25 (g):1 (g)

2.6. Non-Catalytic and Catalytic (Ex Situ) Pyrolysis Setup

The non-catalytic and catalytic pyrolysis experiments were executed at the Biomass and Bioenergy Laboratory, Faculty of Integrated Technologies, Universiti Brunei Darussalam. Pyrolysis with dual reactors (one for biomass and one for catalyst) was used to perform the ex situ catalytic pyrolysis process. Initially, the non-catalytic pyrolysis was run

with this setup without a catalyst at three different temperatures (400, 500, and 600 °C) to get the optimum temperature for the highest bio-oil yield. It was found that the highest production of bio-oil (36.70%) was achieved at 500 °C temperature. That is why the temperature, 500 °C, was maintained for the dual reactors in the catalytic process with a catalyst, keeping all other parameters the same. The catalytic pyrolysis setup for *P. purpureum* grass is shown in Figure 1.

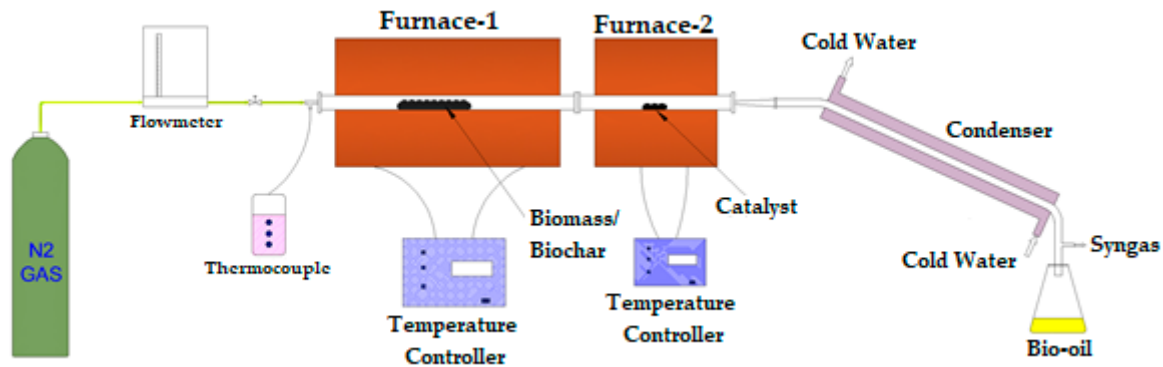


Figure 1. Diagram of the dual fixed-bed catalytic pyrolysis used in this work.

The primary reactor (inner dia-27 mm, and length-500 mm) was used for feedstock and the secondary reactor (inner diameter of 27 mm, and length of 300 mm) was used for the catalyst. Both reactors were made from stainless steel and were inserted horizontally inside the tube furnaces (Gero 300 – 3000, Carbolite Electrical Furnaces, Hope Valley, UK). The primary reactor was filled with 25 g of biomass, while the second reactor was filled with 1 g of catalysts so that the pyrolytic vapor could pass through the catalyst. The catalytic pyrolysis processes for both primary and secondary reactors were carried out at 500 °C, with a heating rate of 25 °C per minute and an N₂ flow rate of 0.5 L per minute. The process was run for 30 min after reaching the final temperature. In order to help the condensable gases, become condensed, cold water was run through the condenser.

The bio-oil was collected from the Erlenmeyer flask, and the biochar was inside the reactor. The syngas was calculated from the mass balance of the biomass feed. The percentage of the pyrolysis products is calculated as per the following Equations (1)–(3) [28].

$$\text{Biochar (wt.\%)} = \left[\frac{w_b}{w_f} \right] \times 100 \quad (1)$$

$$\text{Bio – oil (wt.\%)} = \left[\frac{w_o}{w_f} \right] \times 100 \quad (2)$$

$$\text{Syngas (wt.\%)} = 100 - \{\text{Biochar (wt.\%)} + \text{Bio-oil (wt.\%)}\} \quad (3)$$

where w_f is the weight of feedstock, w_b is the weight of the biochar from the reactor, and w_o is the weight of the bio-oils from the flask and condenser.

The experiments were carried out twice in order to determine the mean value and the reliability of the results. The standard deviation (σ) and the standard error of the mean (σ_e) for the results were calculated as per Equations (4) and (5), respectively [16].

$$\text{standard deviation, } \sigma = \sqrt{\frac{\sum (x - \bar{x})^2}{(n - 1)}} \quad (4)$$

$$\text{standard error of the mean, } \sigma_e = \frac{\sigma}{\sqrt{n}} \quad (5)$$

where x is the individual value for a single experiment, \bar{x} is the mean value of total experiments, and n is the number of experiments conducted.

2.7. Bio-Oils Analysis (GC–MS)

The bio-oils were collected from the conical flask into glass vials and stored in the refrigerator to maintain quality. The oils from the vials were used for further chemical composition analysis through gas chromatography–mass spectrometry (GC–MS). The GC–MS analysis of the bio-oils was conducted at the Faculty of Science, Universiti Brunei Darussalam. The chemical composition of the bio-oils was analyzed using the GC-2010 Plus gas chromatographer–mass spectrometer manufactured by Shimadzu with the Rtx-5MS column (30 m length \times 0.25 mm inner diameter \times 0.25 μ m film thickness). With a 15 mL/min flow rate, helium gas was used as a carrier. The oven was preheated to 50 $^{\circ}$ C for 1 min, then increased to 300 $^{\circ}$ C (10 $^{\circ}$ C/min heating rate) with a 10-min hold time. Using a 3-min solvent cut time and a scanning speed of 1111 amu/s, the ion source and interface temperatures for mass spectroscopy (MS) were 200 and 250 $^{\circ}$ C, respectively. The injector was set at a temperature of 250 $^{\circ}$ C. For analysis, a 1 μ L sample (1000 ppm bio-oil in methanol) was injected into the column. The National Institute of Standards and Technology (NIST 08) [29] mass spectra data library was used to identify chemical compounds based on peak matching. The percentage of the specific compounds in the bio-oil was determined using the region of the calculated peak. For reference and explanation, these findings were examined.

3. Results and Discussions

3.1. Characterizations

The basic characterizations (proximate analysis, ultimate analysis, SEM, EDX, HHV, FTIR, TGA, DTG, and DSC) of this *P. purpureum* grass were explained in previous publications [8,30]. The SEM micrographs of the activated carbon are illustrated in Figure 2a–c at 100, 1000, and 5000 magnifications, respectively.

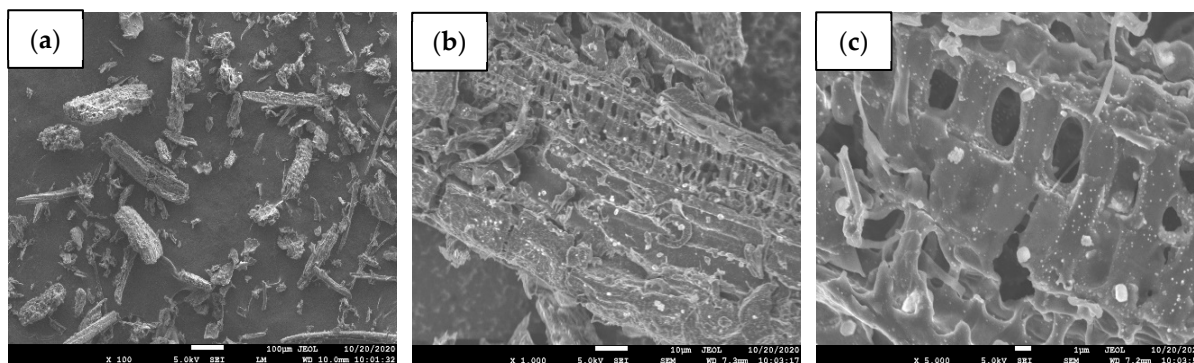


Figure 2. SEM images of the activated carbon at (a) 100, (b) 1000, and (c) 5000 magnifications.

The images exhibit clear pores and specific shapes on the surface of the activated carbon. This is due to the development of internal pores after tars were removed by the activating agents through physiochemical activation. Higher porosity is very important for increasing the surface area of activated carbon [27]. Initially, the microporous structure was developed with the removal of tars and disorganized carbon for the reaction of chemical activating agents (KOH) [31]. Finally, the micro-pore walls were greatly enlarged toward intermediate pores and macro-porosity at higher temperatures [32]. The BET surface area for the activated carbon from *P. purpureum* was achieved as 407 m²/g, which is higher than the values of lawn grass (208 m²/g) [33] and garden grass (21.28 m²/g). The higher surface area and porosity indicate numerous binding sites on the activated carbon [34].

The FTIR diagram and the relevant functional groups of the activated carbon are described in Figure 3. The detected peaks, found at wavenumber 3450 cm^{−1}, were due to the bending of O–H functional groups in the AC [35,36]. Other peaks, achieved at 2935 and 2860 cm^{−1} wavenumbers, were for C–H bond bending in the char [37]. The crests for the wavenumbers of 1652 cm^{−1} were due to the C=C stretching of the activated carbon [38].

The peaks, in the area of 1460 to 1410 cm^{-1} were for stretching of C=O deformation [39]. The peaks, achieved at 880 cm^{-1} wavenumbers, were mainly due to the C=C stretching of the activated carbon elements [40].

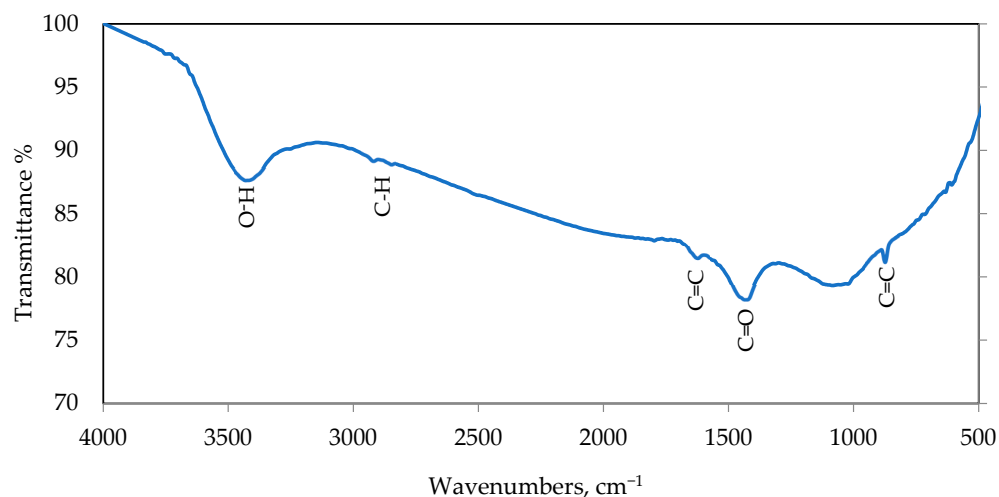


Figure 3. Fourier-transform infrared spectra of activated carbon.

The SEM images of the used activated carbon and the regenerated activated carbon at 1000 magnifications are described in Figure 4. The used AC, -unused RAC-1, used RAC-1 and unused RAC-2 at 1000 magnifications are represented in Figure 4a–d, respectively. The surface of the unused activated carbon is clear, whereas the surface of the used catalyst is blurry and clogged. This is due to coke deposition on the surface of the catalyst during catalytic pyrolysis [41]. It was also found that the pores in the activated carbon were reduced after it was used. In the regenerated activated carbon, the pores become uneven as the walls are broken during the recycling process, and the shape becomes more unstable with the increase in regeneration numbers [42].

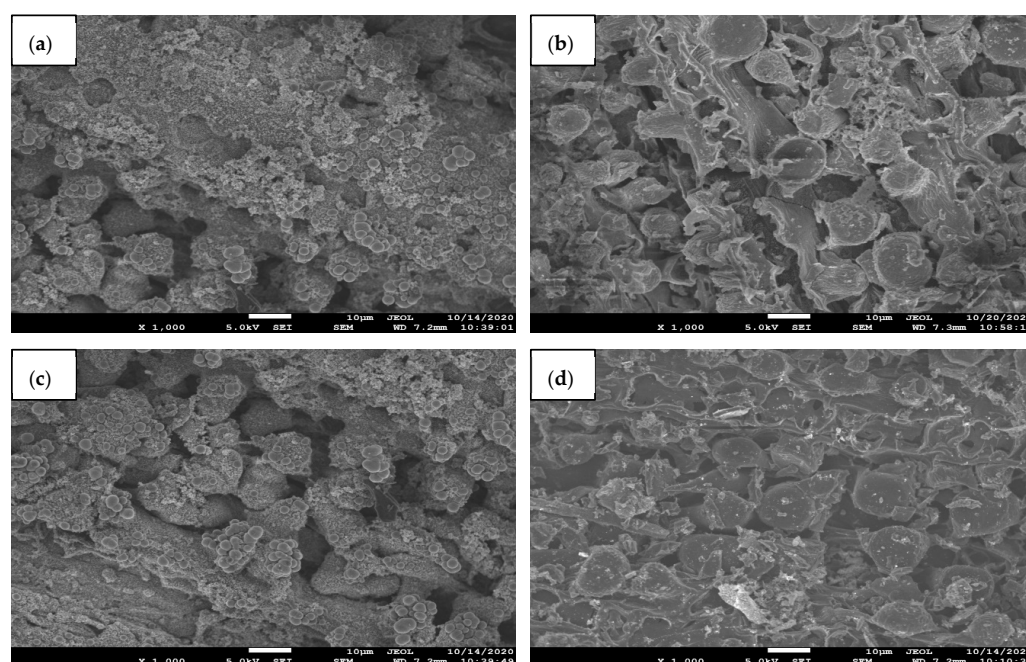


Figure 4. The SEM images of the AC and RAC, (a) used AC, (b) unused RAC-1, (c) used RAC-1, and (d) unused RAC-2 at 1000 magnifications.

3.2. Product Yield (Catalytic and Non-Catalytic Pyrolysis)

For all pyrolysis (catalytic and non-catalytic) processes, the feedstock-to-catalyst weight ratio was constantly maintained at 25:1 (g: g). Some scientists used higher biomass-to-catalyst ratios (1:1, 1:3, and higher) to get the maximum catalytic effects. However, the 25:1 ratio is a practical condition that can be used effectively in the real field. The biomass and catalyst were placed in the reactors according to the following order: biomass (25 g) in the primary reactor, and catalyst (1 g) in the secondary reactor. Firstly, the dual reactor setup was run without any catalyst in the secondary reactor to maintain homogeneity. Secondly, pure AC was used as the catalyst in the second reactor in the catalytic process. The catalysts RAC-1, and RAC-2 were used in the third and fourth runs of the catalytic pyrolysis process, respectively. In all processes, the biomass and the catalyst were placed separately in separate reactors.

The product yield of catalytic and non-catalytic pyrolysis of *P. purpureum* grass is shown in Table 2. The corresponding yields of bio-oil, biochar, and syngas are described in Figure 5. The biochar production from the pyrolysis of non-catalytic and catalytic processes was almost the same due to the ex situ catalytic process, where the primary reactor is fixed for both catalytic and non-catalytic processes with constant operating parameters such as temperature, heating rate, and nitrogen flow rate [43]. The production of the bio-oils and syngas was significantly changed in both the catalytic and non-catalytic pyrolysis processes due to the catalytic effect of the catalyst (Figure 5). The yield of bio-oil decreased and the yield of syngas increased in the catalytic pyrolysis process compared to the non-catalytic process. This is due to catalytic reactions that occurred between pyrolytic vapors and the catalyst when the vapors passed through the catalyst in the secondary reactor [16].

Table 2. The product yield of catalytic and non-catalytic pyrolysis with standard deviation and the standard error of the mean.

Catalyst	Biochar (wt.%)			Bio-Oil (wt.%)			Syngas (wt.%)		
	Mean	σ	σ_e	Mean	σ	σ_e	Mean	σ	σ_e
No catalyst	27.40	0.35	0.25	36.70	0.61	0.43	35.90	0.67	0.47
AC	27.76	0.46	0.33	34.72	0.29	0.21	37.52	0.81	0.57
RAC-1	27.65	0.51	0.36	34.98	0.53	0.37	37.37	0.34	0.24
RAC-2	27.53	0.39	0.28	35.27	0.48	0.34	37.20	0.57	0.40

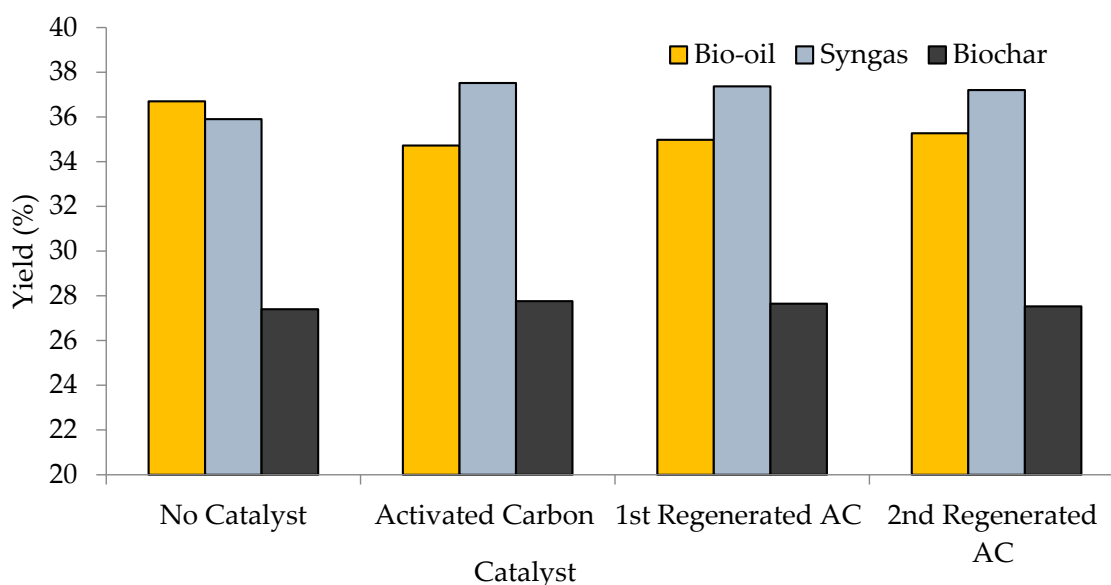


Figure 5. Bio-oil and syngas yield in the catalytic and non-catalytic pyrolysis processes using the dual fixed-bed reactor.

It was found that using raw activated carbon as the catalyst, the bio-oil yield decreased from 36.70% (No-catalyst) to 34.72% (AC) compared to non-catalytic pyrolysis while the syngas yield increased from 35.90% (No-catalyst) to 37.52% (AC). This is due to the reforming reactions that occurred when the pyrolytic vapors passed through the catalyst (activated carbon) in the secondary reactor. In this reaction, the higher molecular compounds were broken into smaller components for the catalyst [44]. The results show a similar trend to other studies of catalytic pyrolysis of glucose-based carbohydrates with activated carbon [45]. The bio-oil yield was higher for the regenerated activated carbon than for raw activated carbon: 34.98% for RAC-1 and 35.27% for RAC-2, respectively. With the catalyst, the syngas yield decreased to 37.37% (RAC-1) and 37.20% (RAC-2). This was because of the reduction in the catalytic activity of the catalyst during the recycling processes [46].

3.3. Bio-Oil Analysis by GC–MS

3.3.1. Non-Catalytic Pyrolysis Process

The chemical components of the bio-oils were examined by gas chromatography–mass spectroscopy. The compound names, chemical formulae, molecular weights, and peak area percentages are listed in Table 3. Organic acids, alcohols, phenols, ketones, furans, esters, nitrogenous compounds, and other oxygenated compounds are the main constituents of non-catalytic bio-oil. A small amount of bromide and sulfur-containing hydrocarbons were also available in the oil. Due to various interference peaks and low concentrations, the chromatogram could not detect several chemicals formed from light volatile materials [47].

It was found from Table 3 that the acidic portion of bio-oils combines acetic acid, ethoxy-, butanoic acid, 4-hydroxy-, maltol, n-decanoic acid, 4-acetylbutyric acid, n-hexadecanoic acid, cis-13-octadecenoic acid, octadecanoic acid, etc. These acids were attributed to the complete decomposition of homo cellulose components of the biomass sample [48]. The percentage of acids must be considered during storage and application as it is among the main ingredients that make the bio-oil more unstable and unusable [49].

The alcohol compounds found in the grass bio-oils were cyclopropyl carbinol, cyclohexanol, 2-methyl-5-(1-methylethyl)-, and 3,3,5,5-tetramethylcyclohexanol where the cyclopropyl carbinol was the highest proportion. The breakdown of cellulose and lignin components present in the raw sample produces these alcohols [50].

There were some portions of aldehydes (2-propenal, 3-phenyl-), esters (butanoic acid, 2-propenyl Ester, 2-propenoic acid, 2-methyl-, 1,2-ethanediyl ester, acetic acid, pentyl ester) and ethers (3,4-dimethylanisole and benzene, 1,2-dimethoxy-) were available in the bio-oils. From the de-carboxylation of cellulose, aldehyde, and esters were produced [51]. Aldehydes are accountable for the aging reactions and poor fuel properties of bio-oils [52]. Reactive compounds such as aldehydes, esters, acids, ketones, and alcohol from higher molecular compounds during storage cause problems such as increased viscosity, phase splitting, and engine nozzle blockage [53].

Furans found in the bio-oils were furan, 2,5-dimethyl-, benzofuran, 2,3-dihydro-, 2-furanmethanol, 2-furancarboxaldehyde, 5-(hydroxymethyl)-, 2-furancarboxaldehyde, 5-methyl-. The dehydration reaction in the quick pyrolysis process produces the furan compounds primarily from hemicellulose and cellulose [54]. Furans are more useful than de-functionalized hydrocarbons, but 2,5-dimethylfuran is unsuitable for bio-oil due to its thermal instability [55]. The food and petroleum sectors frequently employ chemicals derived from furan compounds as organic reagents [56].

The ketone components found were cyclohexanone, 1,2-cyclopentanediol, 3-methyl-, 2-cyclopenten-1-one, 3-ethyl-2-hydroxy-, 2-propanone, 1,1-diphenyl-. The availability and oxidation of hemicellulose in biomass play a major role in the percentage of ketones in bio-oil [51]. It can be difficult to remove water from bio-oil since it can become hydrophilic when more ketones are present [57].

Table 3. Bio-oil components for non-catalytic pyrolysis of *Pennisetum purpureum*.

Ret. Time (min)	Chemical Name	MW	Formula	Peak Area (%)	Chemical Group
3.027	Acetic acid, ethoxy-	104	C ₄ H ₈ O ₃	0.61	Acid
3.172	1H-Pyrazole, 3,5-dimethyl-	96	C ₅ H ₈ N ₂	4.45	Nitrogenous
3.34	2-Furanmethanol	98	C ₅ H ₆ O ₂	3.01	Furans
3.391	2-Propanone, 1-(acetyloxy)-	116	C ₅ H ₈ O ₃	4.29	Misc. Oxygenated
3.758	2-Cyclopenten-1-one, 3-methyl-	96	C ₆ H ₈ O	0.82	Ketones
3.841	Butanoic acid, 4-hydroxy-	104	C ₄ H ₈ O ₃	2.52	Acid
3.977	Cyclohexanone	98	C ₆ H ₁₀ O	2.82	Ketones
4.067	2-Hexanone, 6-hydroxy-	116	C ₆ H ₁₂ O ₂	1.13	Misc. Oxygenated
4.266	2-Furancarboxaldehyde, 5-methyl-	110	C ₆ H ₆ O ₂	0.88	Furans
4.308	2-Cyclopenten-1-one, 3-methyl-	96	C ₆ H ₈ O	0.83	Ketones
4.47	Phenol	94	C ₆ H ₆ O	3.02	Phenolic
4.629	Octanoic acid, 2-amino-	159	C ₈ H ₁₇ NO ₂	2.54	Nitrogenous
4.775	Triethylenediamine	112	C ₆ H ₁₂ N ₂	0.64	Nitrogenous
4.916	2-Cyclopenten-1-one, 2-hydroxy-3-methyl-	112	C ₆ H ₈ O ₂	2.58	Ketones
5.038	2-Propenoic acid, 2-methyl-, 1,2-ethanediy Ester	142	C ₈ H ₁₄ O ₂	0.86	Ester
5.112	Phenol, 2-methyl-	108	C ₇ H ₈ O	1.80	Phenolic
5.293	Phenol, 4-methyl-	108	C ₇ H ₈ O	2.56	Phenolic
5.384	Butanoic acid, 2-propenyl ester	128	C ₇ H ₁₂ O ₂	0.93	Ester
5.428	Phenol, 2-methoxy-	124	C ₇ H ₈ O ₂	1.62	Phenolic
5.606	Cyclopropyl carbinol	72	C ₄ H ₈ O	7.24	Alcohol
5.683	Maltol	126	C ₆ H ₆ O ₃	0.80	Acid
5.724	2-Cyclopenten-1-one, 3-ethyl-2-hydroxy-	126	C ₇ H ₁₀ O ₂	1.90	Ketones
5.929	Phenol, 2,5-dimethyl-	122	C ₈ H ₁₀ O	1.23	Phenolic
5.999	Pentanoic acid, 5-bromo-	181	C ₅ H ₉ BrO ₂	0.32	Bromide
6.095	Phenol, 4-ethyl-	122	C ₈ H ₁₀ O	1.04	Phenolic
6.152	Benzamide, N-hydroxy-	137	C ₇ H ₇ NO ₂	0.23	Nitrogenous
6.206	n-Decanoic acid	172	C ₁₀ H ₂₀ O ₂	0.46	Acid
6.276	Benzyl alcohol	108	C ₇ H ₈ O	0.34	Alcohol
6.346	Phenol, 2-methoxy-4-methyl-	138	C ₈ H ₁₀ O ₂	0.56	Phenolic
6.506	1,2-Benzenediol	110	C ₆ H ₆ O ₂	3.98	Phenolic
6.578	Benzofuran, 2,3-dihydro-	120	C ₈ H ₈ O	3.68	Furans
6.748	2-Furancarboxaldehyde, 5-(hydroxymethyl)-	126	C ₆ H ₆ O ₃	1.63	Furans
6.874	Furan, 2,5-dimethyl-	96	C ₆ H ₈ O	0.22	Furans
6.945	2,5-Hexanedione	114	C ₆ H ₁₀ O ₂	0.52	Ketones
7.061	1,2-Benzenediol, 3-methoxy-	140	C ₇ H ₈ O ₃	1.38	Misc. Oxygenated
7.151	Phenol, 4-ethyl-2-methoxy-	152	C ₉ H ₁₂ O ₂	1.00	Phenolic
7.19	Hydroquinone	110	C ₆ H ₆ O ₂	1.66	Phenolic
7.295	3,3,5,5-Tetramethylcyclohexanol	156	C ₁₀ H ₂₀ O	0.34	Alcohol
7.348	1,2-Benzenediol, 3-methyl-	124	C ₇ H ₈ O ₂	0.89	Phenolic
7.393	1,5-Diacetoxypentane	188	C ₉ H ₁₆ O ₄	0.51	Misc. Oxygenated
7.502	2-Propenal, 3-phenyl-	132	C ₉ H ₈ O	1.29	Aldehyde
7.743	2H-Pyran, tetrahydro-2-methyl-	100	C ₆ H ₁₂ O	0.85	Misc. Oxygenated
7.86	Phenol, 2,6-dimethoxy-	154	C ₈ H ₁₀ O ₃	1.92	Phenolic
7.922	Benzene, 1-methyl-2-(methylthio)-	138	C ₈ H ₁₀ S	0.73	Sulfide
8.02	2-Heptanone, 6-methyl-	128	C ₈ H ₁₆ O	1.00	Ketones
8.088	1-Pentyn-3-ol, 3,4-dimethyl-	112	C ₇ H ₁₂ O	0.56	Misc. Oxygenated
8.172	3-Decanone	156	C ₁₀ H ₂₀ O	0.48	Ketones
8.229	1,3-Benzenediol, 4-ethyl-	138	C ₈ H ₁₀ O ₂	1.11	Phenolic
8.362	3-Buten-2-one, 4-(2,5,6,6-tetramethyl-2-cyclohexen-1-yl)-	206	C ₁₄ H ₂₂ O	0.31	Ketones
8.413	2-Propenoic acid, 2-methyl-, 1,2-ethanediy ester	142	C ₈ H ₁₄ O ₂	0.67	Ester
8.486	1,3-Benzenediol, 4,5-dimethyl-	138	C ₈ H ₁₀ O ₂	0.26	Phenolic
8.636	Acetic acid, ethoxy-	104	C ₄ H ₈ O ₃	1.62	Acid
8.832	3,4-Dimethylanisole	136	C ₉ H ₁₂ O	0.62	Ether
9.139	Bicyclo [2.2.1]heptan-2-one, 5-(acetyloxy)-4,7,7-trimethyl-, endo-	210	C ₁₂ H ₁₈ O ₃	0.21	Ketones
9.667	5-tert-Butylpyrogallol	182	C ₁₀ H ₁₄ O ₃	1.39	Misc. Oxygenated
9.743	Benzene, 1,2-dimethoxy-	138	C ₈ H ₁₀ O ₂	1.61	Ether
9.788	2(3H)-Naphthalenone,4,4a,5,6,7,8-hexahydro-4a-methyl-	164	C ₁₁ H ₁₆ O	3.16	Misc. Oxygenated
10.002	11-Heneicosanone	310	C ₂₁ H ₄₂ O	0.82	Ketones
10.099	3',5'-Dimethoxyacetophenone	180	C ₁₀ H ₁₂ O ₃	0.22	Phenolic
10.598	Pentanoic acid, 4-oxo-, ethyl ester	144	C ₇ H ₁₂ O ₃	0.45	Ester
10.978	4-Acetylbutyric acid	130	C ₆ H ₁₀ O ₃	0.19	Acid
11.522	Glucitol, 6-O-nonyl-	308	C ₁₅ H ₃₂ O ₆	0.19	Misc. Oxygenated
12.356	2-Propanone, 1,1-diphenyl-	210	C ₁₅ H ₁₄ O	0.23	Ketones
12.45	4-Methyl-daphnetin	192	C ₁₀ H ₈ O ₄	0.19	Misc. Oxygenated
14.161	n-Hexadecanoic acid	256	C ₁₆ H ₃₂ O ₂	0.21	Acid
15.951	cis-13-Octadecenoic acid	282	C ₁₈ H ₃₄ O ₂	1.59	Acid
16.129	Octadecanoic acid	284	C ₁₈ H ₃₆ O ₂	0.35	Acid

Another highest proportion of the bio-oils is the miscellaneous oxygenated compounds (15.94%) which were 2-propanone 1-(acetyloxy)-, 2-hexanone, 6-hydroxy-, 1,2-benzenediol 3-methoxy-, 1,5-diacetoxypentane, 2H-pyran, tetrahydro-2-methyl-, 5-tert-butylpyrogallol, etc. High-oxygenate bio-oils are not recommended as motor fuel due to their corrosiveness and poor energy content [58].

The bio-oil contains a high amount of nitrogenous components, which were 1H-pyrazole, 3,5-dimethyl-, octanoic acid, 2-amino-, triethylenediamine, benzamide, N-hydroxy-. Nitrogenous components are problematic for sedimentation and lower the thermal stability of the fuel [59]. Nitrogenous compounds also harm the environment because they produce noxious gas during burning [60].

The 1,2-benzenediol, phenol, phenol 2-methyl, phenol 4-methyl, phenol, 2-6-dimethoxy, and 1, 3-benzenediol 4-ethyl combinations were the main phenolic components of the bio-oils for the non-catalytic pyrolysis. The lignin in the biomass is mostly broken down to create the phenolic chemicals [61]. Phenols are important for producing plastics, pharmaceuticals, cosmetics, and high-value-added products [55].

This oil contains a small portion of bromide acid (pentanoic acid, 5-bromo-) and sulfide hydrocarbon (benzene, 1-methyl-2-(methylthio)-). As sulfur may cause heart disease, asthma, respiratory conditions, and other ailments, its presence in liquid fuels risks automobiles [62]. The bromine mix oil can produce methyl bromide during combustion, contributing to stratospheric ozone depletion [63].

3.3.2. Catalytic Pyrolysis Process (AC, RAC-1, and RAC-2)

The chemicals and their bio-oil groups in the catalytic pyrolysis with activated carbon and regenerated activated carbon (AC, RAC-1, and RAC-2) are described in Table 4. By comparison with non-catalytic pyrolysis, the percentage of acid was effectively reduced for the catalysts of activated carbon and regenerated activated carbon. This was due to the cracking of the acidic components into different hydrocarbons under the effect of the catalyst [64]. The acidic components in these bio-oils for catalytic pyrolysis were propanoic acid, benzenoacetic acid, 3,4-dihydroxy-, and nonanoic acid. Among the catalysts, the percentages of acids were lowest for the raw activated carbon and increased with the cycle of regenerated activated carbons. This was mainly because of the reduced catalytic performance of the regenerated activated carbons with the increased number of reaction cycles [46].

The alcohol compounds were increased for the catalysts than the non-catalytic pyrolysis due to the conversion of carboxylic acids into alcohols by hydrotreating [65]. The major components of the alcohol for the AC and RAC were 2-butene-1,4-diol, 3-hepten-1-ol, benzyl alcohol, 4-methylcatechol, 3-methoxybenzyl alcohol, 2-nonen-1-ol, and isborneol. With the regeneration of activated carbons, the alcohol yield was reduced but still higher than the non-catalytic bio-oil. That means there was still the presence of active sites in catalysts after regeneration [66].

The amount of aldehyde, ester, and ether was decreased for catalytic pyrolysis rather than non-catalytic pyrolysis. This is due to the breakdown of catalytic vapors with catalysts through decarbonylation and decarboxylation [67]. Less aldehyde, ester, and ether are effective for storing and allocating bio-oils [53].

The number of furans was increased for catalytic than non-catalytic pyrolysis where the chemicals were furan, tetrahydro-, 2-furanmethanol, 2-furanol, tetrahydro-, benzofuran, 2,3-dihydro-, 2-coumaranone, etc. Similarly, the ketones were increased with the components of 2-cyclopenten-1-one, 2-cyclopenten-1-one, 3-methyl-, butyrolactone, 2-cyclopenten-1-one, 2-methyl-, cyclohexanone, butyrolactone, 1,2-cyclopentanedione, 3-methyl-, 2-cyclopenten-1-one, 3-ethyl-2-hydroxy-, etc. The number of furans and ketones was increased due to the further conversion of pyrolytic vapor through dehydration, oligomerization, and rearrangement reactions. The increasing trend of furan and ketone production with activated carbon catalysts is similar to the catalytic pyrolysis of Douglas fir with activated carbon [67]. Among the catalysts, the yield of furan was lower for RAC-2 than AC, but

ketones were higher for RAC-2 than AC. This was due to the reduction in the catalytic activity of regenerated activated carbons with cycles [46].

Table 4. Bio-oil components of catalytic pyrolysis process (AC, RAC-1, and RAC-2).

Ret. Time (min)	Chemical Name	MW	Chemical Formula	AC	RAC-1	RAC-2	Chemical Group
				Area (%)	Area (%)	Area (%)	
3.029	Propanoic acid	74	C ₃ H ₆ O ₂	1.43	5.40	1.42	Acid
3.146	2-Cyclopenten-1-one	82	C ₅ H ₆ O	5.05	1.88	0.92	Ketones
3.245	Furan, tetrahydro-	72	C ₄ H ₈ O	1.26	2.70	2.85	Furans
3.337	2-Furanmethanol	98	C ₅ H ₆ O ₂	3.36	2.40	3.99	Furans
3.407	2-Butene-1,4-diol	88	C ₄ H ₈ O ₂	2.84	2.51	0.00	alcohol
3.524	3-Hepten-1-ol	114	C ₇ H ₁₄ O	1.32	4.42	3.85	alcohol
3.618	Furan, 2-methyl-	82	C ₅ H ₆ O	0.10	3.44	0.00	Furans
3.675	2-Furanmethanol	98	C ₅ H ₆ O ₂	0.33	1.85	2.06	Furans
3.781	2-Cyclopenten-1-one, 3-methyl-	96	C ₆ H ₈ O	0.86	0.89	3.37	Ketones
3.847	Phenol, 2-methyl-	108	C ₇ H ₈ O	2.34	2.04	1.84	Phenolic
3.917	Phenol	94	C ₆ H ₆ O	0.87	1.51	0.00	Phenolic
3.962	2-Cyclopenten-1-one, 2-methyl-	96	C ₆ H ₈ O	1.94	1.48	1.80	Ketones
4.141	Butyrolactone	86	C ₄ H ₆ O ₂	0.36	2.69	1.98	Ketones
4.276	Cyclohexanone	98	C ₆ H ₁₀ O	0.85	1.01	3.53	Ketones
4.313	2-Cyclopenten-1-one, 3-methyl-	96	C ₆ H ₈ O	0.93	2.24	1.51	Ketones
4.449	Phenol	94	C ₆ H ₆ O	12.83	12.19	2.68	Phenolic
4.664	2-Propanone, 1-(acetyloxy)-	116	C ₅ H ₈ O ₃	0.59	3.37	2.83	Misc. Oxygenated
4.883	1,2-Cyclopentanedione, 3-methyl-	112	C ₆ H ₈ O ₂	2.01	0.89	1.03	Ketones
4.984	2-Cyclopenten-1-one, 2-hydroxy-3-methyl-	112	C ₆ H ₈ O ₂	0.20	2.13	1.91	Ketones
5.025	2-Cyclopenten-1-one, 2,3-dimethyl-	110	C ₇ H ₁₀ O	0.12	0.68	1.03	Ketones
5.091	Benzyl alcohol	108	C ₇ H ₈ O	2.32	2.19	2.44	Alcohol
5.339	Phenol, 2-methyl-	108	C ₇ H ₈ O	4.86	4.15	2.55	Phenolic
5.408	2-Cyclopenten-1-one, 3-ethyl-2-hydroxy-	126	C ₇ H ₁₀ O ₂	0.11	2.40	1.04	Ketones
5.466	Phenol, 2-ethyl-	122	C ₈ H ₁₀ O	0.28	1.45	3.27	Phenolic
5.671	2-Cyclopenten-1-one, 3-ethyl-2-hydroxy-	126	C ₇ H ₁₀ O ₂	1.89	1.23	2.25	Ketones
5.798	Phenol, 2-ethyl-	122	C ₈ H ₁₀ O	0.20	0.80	0.80	Phenolic
5.907	Phenol, 2,5-dimethyl-	122	C ₈ H ₁₀ O	0.95	1.96	2.25	Phenolic
6.059	Phenol, 4-ethyl-	122	C ₈ H ₁₀ O	2.54	1.85	1.73	Phenolic
6.177	Phenol, 2,6-dimethyl-	122	C ₈ H ₁₀ O	0.13	1.04	0.85	Phenolic
6.243	2,4-Imidazolidinedione, 5,5-dimethyl-	128	C ₅ H ₈ N ₂ O ₂	0.10	0.78	0.62	Nitrogenous
6.39	Benzofuran, 2,3-dihydro-	120	C ₈ H ₈ O	10.06	2.57	3.89	Furans
6.533	1,2-Benzenediol	110	C ₆ H ₆ O ₂	4.62	1.84	2.09	Phenolic
6.685	Resorcinol monoacetate	152	C ₈ H ₈ O ₃	2.40	1.22	1.74	Misc. Oxygenated
6.852	2-Coumaranone	134	C ₈ H ₆ O ₂	0.27	0.57	0.56	Furans
6.95	1,2-Benzenediol, 4-methyl-	124	C ₇ H ₈ O ₂	1.89	1.34	0.92	Phenolic
7.01	Caprolactam	113	C ₆ H ₁₁ NO	1.40	1.56	2.27	Nitrogenous
7.068	Hydroquinone	110	C ₆ H ₆ O ₂	2.61	0.84	1.39	Phenolic
7.243	4-Methylcatechol	124	C ₇ H ₈ O ₂	3.63	1.45	1.99	Alcohol
7.395	Phenol, 4-ethyl-2-methoxy-	152	C ₉ H ₁₂ O ₂	0.48	0.46	1.02	Phenolic
7.535	Benzoic acid, 2-hydroxy-5-methyl-, methyl ester	166	C ₉ H ₁₀ O ₃	0.34	0.97	0.71	Ester
7.602	2-Nonen-1-ol	142	C ₉ H ₁₈ O	0.18	0.27	0.99	Alcohol
7.648	1,3-Benzenediol, 2-methyl-	124	C ₇ H ₈ O ₂	0.57	0.27	0.35	Phenolic
7.74	3-Methoxybenzyl alcohol	138	C ₈ H ₁₀ O ₂	1.31	0.26	0.44	alcohol
7.849	1,4-Benzenediol, 2-methyl-	124	C ₇ H ₈ O ₂	0.39	0.43	2.10	Phenolic
7.899	Benzofuran, 2-methyl-	132	C ₉ H ₈ O	0.26	0.80	0.66	Furans
7.938	Benzaldehyde, 4-hydroxy-	122	C ₇ H ₆ O ₂	0.21	0.40	0.51	Aldehyde
8.153	1,3-Benzenediol, 4-ethyl-	138	C ₈ H ₁₀ O ₂	2.15	0.24	1.84	Phenolic
8.281	Ethanone, 1-(3-hydroxyphenyl)-	136	C ₈ H ₈ O ₂	0.18	0.46	0.57	Ketones
8.413	1,3-Benzenediol, 4,5-dimethyl-	138	C ₈ H ₁₀ O ₂	0.07	0.22	0.53	Phenolic
8.558	Benzoic acid, ethyl ester	150	C ₉ H ₁₀ O ₂	0.44	0.15	1.70	Ester
8.752	Phenol, 2,3,6-trimethyl-	136	C ₉ H ₁₂ O	0.76	0.10	0.47	Phenolic
8.846	Isoborneol	154	C ₈ H ₁₀ O ₂	0.17	0.01	0.53	Alcohol
8.942	Phenol, 2,3,6-trimethyl-	136	C ₉ H ₁₂ O	0.13	0.00	1.19	Phenolic
9.155	Benzeneacetic acid, 3,4-dihydroxy-	168	C ₈ H ₈ O ₄	0.10	0.00	1.03	Acid
9.256	Nonanoic acid	158	C ₉ H ₁₈ O ₂	1.70	0.00	2.72	Acid
9.668	2(3H)-Naphthalenone,4,4a,5,6,7,8-hexahydro-4a-methyl-	164	C ₁₁ H ₁₆ O	0.48	0.01	0.84	Misc. Oxygenated
10.18	4-Acetylbutyric acid	130	C ₆ H ₁₀ O ₃	0.23	0.00	0.58	Acid

The nitrogenous and oxygenated compounds were reduced tremendously due to the use of catalysts rather than no catalyst because activated carbon can provide increased selectivity for direct oxygen removal with lower hydrogen consumption [19]. This may also occur for the deoxygenation during catalytic pyrolysis through decarbonylation, decarboxylation, and dehydration mechanisms [68]. For AC, RAC-1, and RAC-2, the yield of nitrogenous and oxygenated compounds was increased gradually due to the gradual decrease in the catalyst activity for some irreversible poisoning [69].

The major change was achieved in the yield of phenolic compounds for catalyst rather than non-catalyst. The amounts of phenolic were increased for all catalysts, and the compounds were phenol, 2-methyl-, phenol, 4-ethyl-, 1,2-benzenediol, hydroquinone, 1,2-benzenediol, 4-methyl-, phenol, 2,3,6-trimethyl-, etc. The production of phenol was higher mainly for converting unstable acids and oxygenated compounds into stable phenolics through the reaction between $-C=O$ and $-OH$ functional groups of the activated carbon with the pyrolytic vapor [64]. The synthesis of activated carbon with the KOH contains an enormous number of active functional groups $-C=O$, $O-H$, $C=C$, and $C-H$ [39], which was supporting catalytic activity. The percentage of phenolic was reduced for the higher number of regenerated activated carbon to decrease the catalytic activity with the number of recycling [70].

3.4. Comparison of Major Bio-Oil Chemicals from Catalytic and Non-Catalytic Pyrolysis

The chemical groups of the bio-oils from the GC-MS results for the non-catalytic and catalytic pyrolysis processes are summarized in Table 5. The total amount of chemicals accounted for 90%, as some of the light volatile compounds were not detected in the chromatogram due to multiple peaks and low concentrations.

Table 5. Summary of the chemical groups of the bio-oils from GC-MS in catalytic and non-catalytic pyrolysis.

Chemical Groups	No Catalyst	Activated Carbon (AC)	1st Regenerated AC (RAC-1)	2nd Regenerated AC (RAC-2)
Acid	8.34	3.46	5.40	5.75
Alcohol	7.91	11.78	11.10	10.23
aldehyde	1.29	0.21	0.40	0.51
Ester	2.91	0.78	1.12	2.41
Ether	2.23	-	-	-
Furans	9.42	15.65	14.33	14.01
Ketones	12.51	14.49	17.99	20.94
Nitrogenous	7.86	1.50	2.34	2.90
Misc. Oxygenated	13.65	3.47	4.60	5.41
Phenolic	22.88	38.66	32.72	27.84
Bromide	0.32	-	-	-
Sulfide	0.73	-	-	-
Total (%)	90.05	90.00	90.00	90.00

The overall performance of activated carbon and regenerated activated carbons was promising for improving the quality of bio-oil for catalytic pyrolysis over the non-catalytic pyrolysis process. The major chemicals were phenolic, alcohol, furans, and ketones for both processes. The catalysts, activated carbon, and regenerated activated carbon, significantly affirmed the reduction in the acidic, aldehyde, oxygenated, and nitrogenous composites in the bio-oils. In the non-catalytic process, there were a small number of halogens and sulfide components in the bio-oils, which disappeared in the catalytic pyrolysis for de-sulfurization and de-halogenation reactions with pyrolytic vapor and catalysts [71]. Before applying the oil to the fuel engine, the removal of halogens and sulfides from bio-oils is highly important because these compounds can generate hazardous gases for the environment [72,73].

3.4.1. Comparison of Major Chemical Groups of Bio-Oils

The production of phenols and alcohols in the bio-oils for the catalytic and non-catalytic pyrolysis processes is described in Figure 6a. The overall yield of phenolic com-

pounds was higher in the catalytic pyrolysis process than in the non-catalytic pyrolysis process. The highest amount of phenols was produced for the composition of the catalysts AC, followed by RAC-1, RAC-2, and no catalyst. The increase in phenols was related to the decrease in oxygenated compounds and acids for catalytic effects [67].

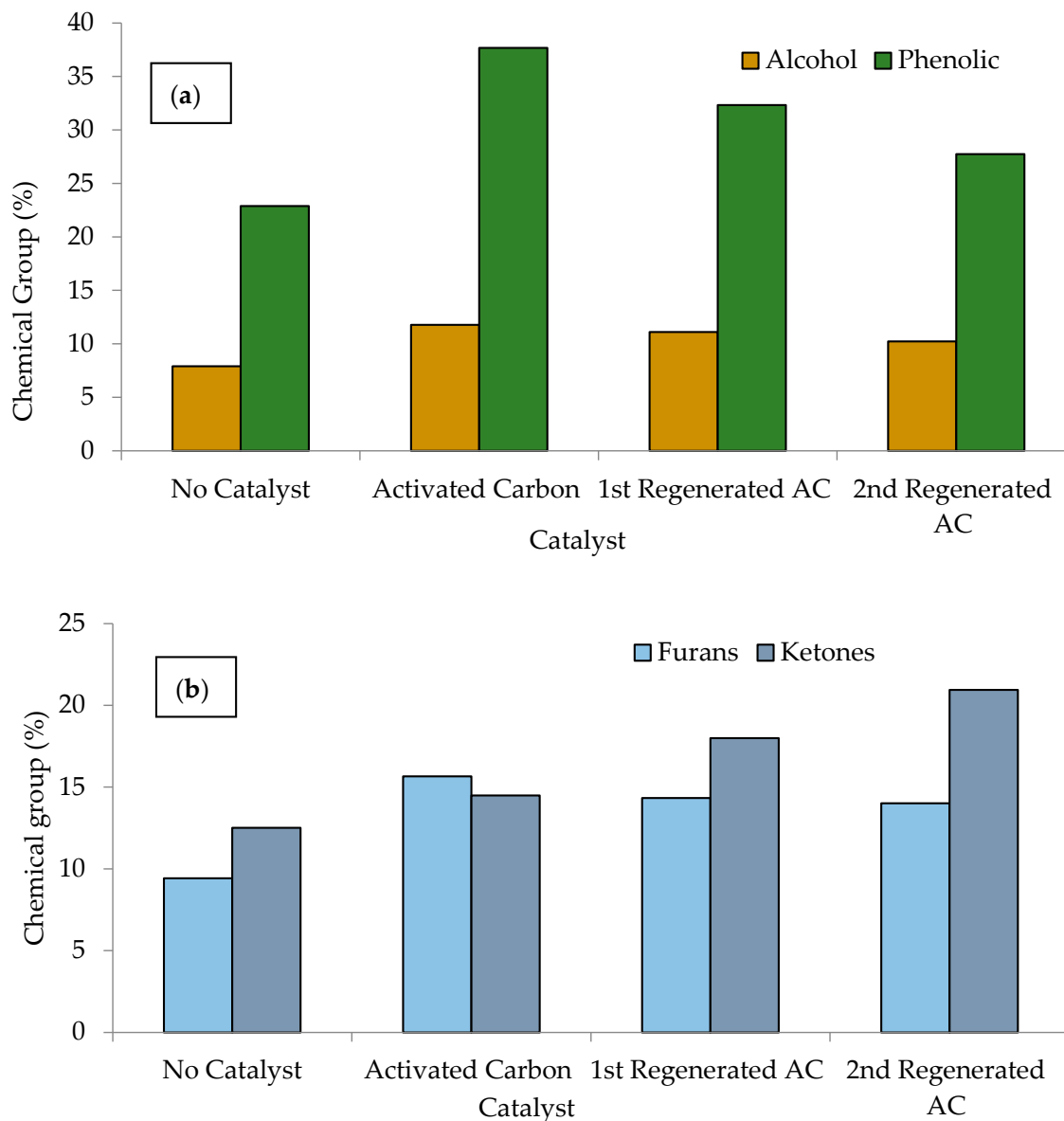


Figure 6. (a) Phenolic and alcohols, (b) furans, and ketones in the bio-oils for the catalyst and non-catalyst using the dual fixed-bed reactor.

The alcohol components in the bio-oils were also higher for the catalytic than the non-catalytic pyrolysis process. The maximum amount of phenols was found for AC for the raw and blended catalyst, followed by RAC-1, RAC-2, and no catalyst. The amount of alcohol was increased due to the reformation of acidic components with the action of an activated carbon catalyst [74]. Higher alcohols are essential for upgraded biofuel production [60]. The production of furans and ketones in the bio-oils for the catalytic and non-catalytic pyrolysis processes is illustrated in Figure 6b. Compared to non-catalyst, the number of furans was higher for raw activated carbon and regenerated activated carbon. The amount of furans depends on the oligomerization and rearrangement reactions [67]. Furans in the bio-oils are considered important components for high-value-added chemical products [60]. A higher amount of ketones was found for the catalyst of RAC-2 and a lower amount of ketones

was achieved for no catalyst. Ketonization is important to reduce the detrimental effects of acids in bio-oils [75]. The production of the ketone is dependent on the decarbonylation reactions of the pyrolytic vapor with the structure of the catalysts [67,76].

The production of acids, nitrogenous compounds, and miscellaneous oxygenated compounds in the bio-oils for the catalytic and non-catalytic pyrolysis processes is described in Figure 7. The acidic, nitrogenous, and miscellaneous oxygenated compounds were reduced significantly for all the catalysts. The lowest yield of acidic components was found for the catalyst, AC, followed by RAC-1, RAC-2, and no catalyst. The acidic components were reduced due to the hydrocracking, dehydration, hydrogenation, and deoxygenation reactions of catalysts to enhance the quality of bio-oils [77].

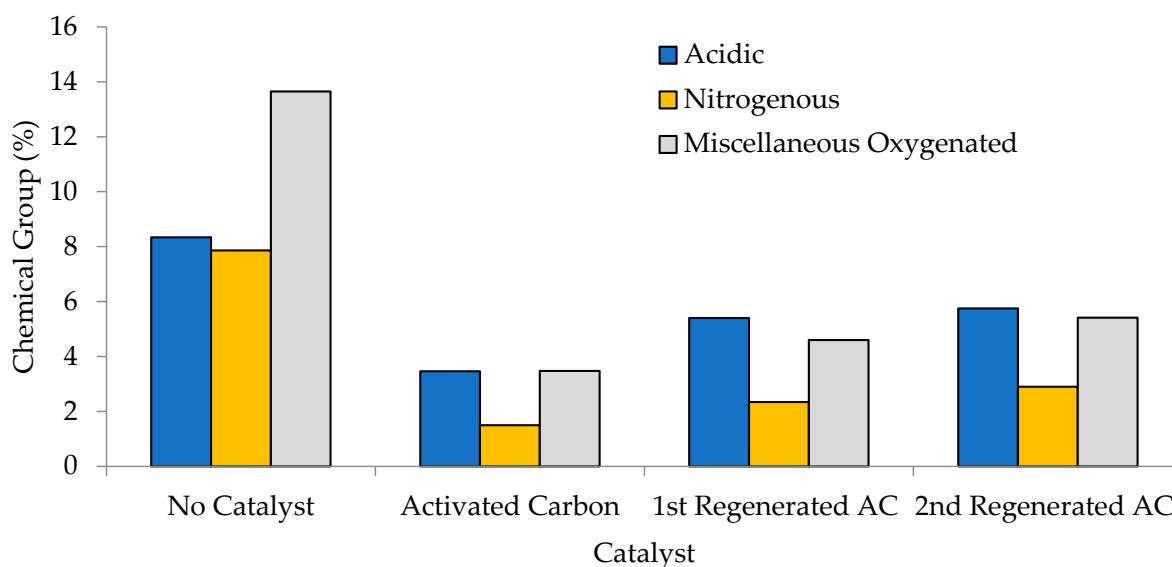


Figure 7. Acids, nitrogenous, and miscellaneous oxygenated compounds in the bio-oils for the catalytic and non-catalytic pyrolysis process from the dual reactor.

Similar to acid reduction, the nitrogenous compounds were the lowest for the catalyst AC and the highest for no catalyst. Additionally, the miscellaneous oxygenated compounds were the lowest for the catalyst of AC followed by RAC-1, RAC-2, and no catalyst. The reduction in nitrogenous and miscellaneous oxygenated compounds occurred due to the reformation reaction with the pyrolytic vapor and catalysts [67].

3.4.2. Comparison of Some Specific Chemicals of Bio-Oils

The production of the chemicals, phenol (carbolic acid) and phenol, 2-methyl- (o-Cresol) in the bio-oils for the catalytic and non-catalytic pyrolysis process is described in Figure 8a. Compare to non-catalyst, the amount of phenol was higher for the catalysts AC and RAC-1. The production of phenol was higher for the active functional groups ($-C=O$ and $-OH$) of the activated carbon [64]. Phenol is a potential precursor to produce plastics, polycarbonates, Bakelite, epoxies, nylon, herbicides, detergents, and various pharmaceutical drugs [78].

Phenol, 2-methyl- in the bio-oils was also higher for the catalytic than the non-catalytic pyrolysis process. The highest amount of phenol, 2-methyl- was achieved for the catalyst AC, RAC-1, and RAC-2 as the production of phenol mainly depends on the active functional groups of the activated carbon [64]. Phenol, 2-methyl- or o-Cresol is the precursor of herbicides and pharmaceutical intermediates [79].

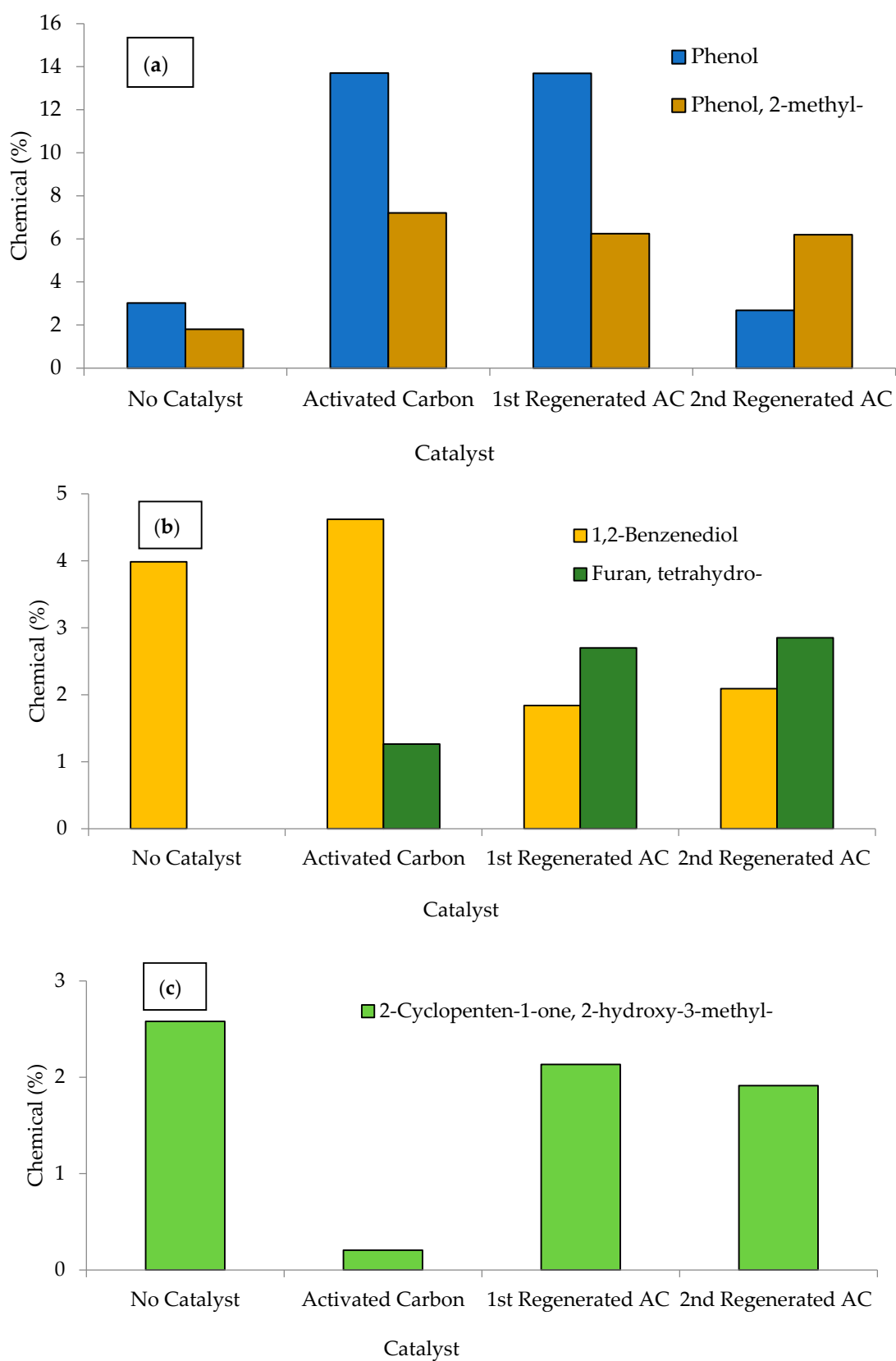


Figure 8. (a) Production of phenol and phenol, 2-methyl-, (b) furan, tetrahydro- and 1,2-benzenediol (catechol), and (c) 2-cyclopenten-1-one, 2-hydroxy-3-methyl- for the catalytic and non-catalytic pyrolysis from the dual reactor.

The 1,2-benzenediol (catechol) percentages and furan tetrahydro- in the bio-oils for the catalytic and non-catalytic pyrolysis process are depicted in Figure 8b. The highest amount of 1,2-benzenediol (catechol) was found for the catalyst AC and gradually decreased for RAC-1 and RAC-2. The catechol or 1,2-benzenediol is used mainly to manufacture pesticides and as a precursor of perfumes and pharmaceuticals [80]. Furan, tetrahydro- was not available in the non-catalytic pyrolysis, whereas it produced a significant amount in the catalytic process and gradually increased for AC, RAC-1, and RAC-2. The main application of furan, tetrahydro- is as a polymerization agent and industrial solvent for polyvinyl chloride and in varnishes [81]. The yield of 2-cyclopenten-1-one, 2-hydroxy-3-methyl- in the bio-oils for the catalytic and non-catalytic pyrolysis process is illustrated in Figure 8c. For the upgraded bio-oils, the amount of 2-cyclopenten-1-one, 2-hydroxy-3-methyl- should be lower [82]. The lowest amount of 2-cyclopenten-1-one, 2-hydroxy-3-methyl- was found for the catalyst AC compared to non-catalytic pyrolysis.

4. Conclusions

In light of all of the findings presented in this thesis, it is notable that the novel technique for producing energy from biomass presented here has the potential to pave the way for new directions in renewable energy development. In this research, the invasive *P. purpureum* grass was used to produce biochar, bio-oil, and syngas through the non-catalytic and catalytic pyrolysis processes. The biochar was converted into activated carbon (AC) through physiochemical activation with potassium hydroxide (KOH) to be used as the catalyst in the catalytic pyrolysis process. This synthesized AC contained a large surface area and a high number of active functional groups (-C=O, O-H, C=C, and C-H), which effectively increased the catalytic activity. In the catalytic pyrolysis with activated carbon, the qualities of the bio-oils were significantly improved compared to the non-catalytic process by enhancing the stable chemicals (phenolic, alcohol, furans, ketones, esters, and aromatic compounds) while reducing the number of unstable chemicals (acidic, aldehydes, nitrogenous, and miscellaneous oxygenated compounds). Among the stable components, the highest amount of phenolic compounds (38.66%) was produced from the AC catalyst, and the lowest amount (22.88%) was from the non-catalyst. This was because of the higher number of active functional groups (-C=O and -OH) in activated carbon, which were effective for phenolic production. The alcohol components were higher for all catalysts than no catalyst, where the highest amount was found for catalyst AC (11.78%), and the lowest (7.91%) was for no catalyst. This was because of the reformation of acidic components into alcohols by the activated carbon catalyst. The highest amount of furans also showed a similar trend: highest for AC (15.65%) and lowest for without catalyst (9.42%). However, the highest amount of ketones was achieved by the catalyst RAC-2 (20.94%) rather than no catalyst (12.51%). This higher amount of ketones produced from the regenerated activated carbons was an economical method for reusing the catalyst, and it is also important to reduce the acidic effect of the bio-oils.

The acidic, nitrogenous, and miscellaneous oxygenated compounds were reduced significantly by using a catalyst, where the minimum amount was found for AC due to the active sites and higher surface area. The precursor of medicines and herbicides, phenol, 2-methyl- or o-Cresol, was produced at the highest levels for the catalyst AC and gradually declined for RAC-1, RAC-2, and non-catalyst. Furan, tetrahydro-, an industrial solvent, was not found in the non-catalytic process but was found in the catalytic process, where the maximum was for AC, and decreased gradually for RAC-1, and RAC-2. In conclusion, the activated carbon from *P. purpureum* is an effective catalyst for the catalytic pyrolysis of *P. purpureum* to upgrade the quality of the bio-oils, and the regenerated activated carbon also showed better output as the catalyst than non-catalysts. Future research can be executed for different biomass to catalyst ratios with different operating conditions and several regenerations of activated carbons for economical and effective outputs.

Supplementary Materials: The following supporting information can be downloaded at: <https://www.mdpi.com/article/10.3390/su15097628/s1>, Figure S1: Biomass sample preparation diagram. Figure S2: The preparation diagram of activated carbon.

Author Contributions: Conceptualization M.S.R. and S.A.; methodology, M.S.R., S.A., K.K., A.K. and K.Z.B.; formal analysis, M.S.R., H.R. and M.S.I.; writing—original draft preparation, M.S.R., S.A., K.K., A.K., K.Z.B., J.T., F.J., M.S.A.B. and A.K.A.; writing—review and editing, M.S.R., H.R. and M.S.I.; supervision, S.A. and M.S.I.; funding acquisition, M.S.I. All authors have read and agreed to the published version of the manuscript.

Funding: This research received no external funding.

Informed Consent Statement: Not applicable.

Data Availability Statement: Data would be available on a reasonable request from the corresponding author(s).

Acknowledgments: The authors would like to acknowledge, Universiti Brunei Darussalam, Brunei, Prince of Songkla University, Thailand, L.N. Gumilyov Eurasian National University, Kazakhstan, and Bangladesh University of Engineering and Technology for supporting this work. The authors are also grateful to Nur Farah Izzan Hj Mohamed Jefri for helping in this work.

Conflicts of Interest: The authors declare no conflict of interest.

References

1. Afroze, S.; Reza, M.S.; Amin, M.R.; Taweekun, J.; Azad, A.K. Progress in Nanomaterials Fabrication and Their Prospects in Artificial Intelligence towards Solid Oxide Fuel Cells: A Review. *Int. J. Hydrogen Energy* **2022**, *in press*. [[CrossRef](#)]
2. Li, G.; Hu, R.; Wang, N.; Yang, T.; Xu, F.; Li, J.; Wu, J.; Huang, Z.; Pan, M.; Lyu, T. Cultivation of Microalgae in Adjusted Wastewater to Enhance Biofuel Production and Reduce Environmental Impact: Pyrolysis Performances and Life Cycle Assessment. *J. Clean. Prod.* **2022**, *355*, 131768. [[CrossRef](#)]
3. Reza, M.S.; Ahmad, N.B.H.; Afroze, S.; Taweekun, J.; Sharifpur, M.; Azad, A.K. Hydrogen Production from Water Splitting Through Photocatalytic Activity of Carbon-Based Materials, A Review. *Chem. Eng. Technol.* **2023**, *46*, 420–434. [[CrossRef](#)]
4. Li, G.; Hao, Y.; Yang, T.; Xiao, W.; Pan, M.; Huo, S.; Lyu, T. Enhancing Bioenergy Production from the Raw and Defatted Microalgal Biomass Using Wastewater as the Cultivation Medium. *Bioengineering* **2022**, *9*, 637. [[CrossRef](#)] [[PubMed](#)]
5. Panwar, N.L.; Kaushik, S.C.; Kothari, S. Role of Renewable Energy Sources in Environmental Protection: A Review. *Renew. Sustain. Energy Rev.* **2011**, *15*, 1513–1524. [[CrossRef](#)]
6. Van Meerbeek, K.; Appels, L.; Dewil, R.; Calmeyn, A.; Lemmens, P.; Muys, B.; Hermy, M.; Van Meerbeek, K.; Appels, L.; Dewil, R.; et al. Biomass of Invasive Plant Species as a Potential Feedstock for Bioenergy Production. *Biofuels Bioprod. Biorefining* **2015**, *9*, 273–282. [[CrossRef](#)]
7. Pimentel, D.; Zuniga, R.; Morrison, D. Update on the Environmental and Economic Costs Associated with Alien-Invasive Species in the United States. *Ecol. Econ.* **2005**, *52*, 273–288. [[CrossRef](#)]
8. Reza, M.S.; Islam, S.N.; Afroze, S.; Abu Bakar, M.S.; Sukri, R.S.; Rahman, S.; Azad, A.K.; Bakar, M.S.A.; Sukri, R.S.; Rahman, S.; et al. Evaluation of the Bioenergy Potential of Invasive *Pennisetum Purpureum* through Pyrolysis and Thermogravimetric Analysis. *Energy Ecol. Environ.* **2020**, *5*, 118–133. [[CrossRef](#)]
9. Zaman, C.Z.; Pal, K.; Yehye, W.A.; Sagadevan, S.; Shah, S.T.; Adebisi, G.A.; Marliana, E.; Rafique, R.F.; Johan, R. Bin Pyrolysis: A Sustainable Way to Generate Energy from Waste. In *Pyrolysis*; InTech: London, UK, 2017; pp. 1–35.
10. Reza, M.S.; Taweekun, J.; Afroze, S.; Siddique, S.A.; Islam, M.S.; Wang, C.; Azad, A.K. Investigation of Thermochemical Properties and Pyrolysis of Barley Waste as a Source for Renewable Energy. *Sustainability* **2023**, *15*, 1643. [[CrossRef](#)]
11. Elliott, D.C. Historical Developments in Hydroprocessing Bio-Oils. *Energy Fuels* **2007**, *21*, 1792–1815. [[CrossRef](#)]
12. Radenahmad, N.; Md Sumon, R.; Muhammad, S.; Abu, B.; Azad, A.K. Thermochemical Characterization of Rice Husk (*Oryza Sativa* Linn) for Power Generation. *ASEAN J. Chem. Eng.* **2020**, *20*, 184–195. [[CrossRef](#)]
13. Balat, M. An Overview of the Properties and Applications of Biomass Pyrolysis Oils. *Energy Sources Part A Recover. Util. Environ. Eff.* **2011**, *33*, 674–689. [[CrossRef](#)]
14. Qiu, B.; Tao, X.; Wang, J.; Liu, Y.; Li, S.; Chu, H. Research Progress in the Preparation of High-Quality Liquid Fuels and Chemicals by Catalytic Pyrolysis of Biomass: A Review. *Energy Convers. Manag.* **2022**, *261*, 115647. [[CrossRef](#)]
15. Kan, T.; Strezov, V.; Evans, T.; He, J.; Kumar, R.; Lu, Q. Catalytic Pyrolysis of Lignocellulosic Biomass: A Review of Variations in Process Factors and System Structure. *Renew. Sustain. Energy Rev.* **2020**, *134*, 110305. [[CrossRef](#)]
16. Syazaidah, I.; Abu Bakar, M.S.; Reza, M.S.; Azad, A.K. Ex-Situ Catalytic Pyrolysis of Chicken Litter for Bio-Oil Production: Experiment and Characterization. *J. Environ. Manag.* **2021**, *297*, 113407. [[CrossRef](#)]
17. Ennaert, T.; Van Aelst, J.; Dijkmans, J.; De Clercq, R.; Schutyser, W.; Dusselier, M.; Verboekend, D.; Sels, B.F. Potential and Challenges of Zeolite Chemistry in the Catalytic Conversion of Biomass. *Chem. Soc. Rev.* **2016**, *45*, 584–611. [[CrossRef](#)]

18. Bu, Q.; Lei, H.; Wang, L.; Yadavalli, G.; Wei, Y.; Zhang, X.; Zhu, L.; Liu, Y. Biofuel Production from Catalytic Microwave Pyrolysis of Douglas Fir Pellets over Ferrum-Modified Activated Carbon Catalyst. *J. Anal. Appl. Pyrolysis* **2015**, *112*, 74–79. [CrossRef]
19. De, S.; Saha, B.; Luque, R. Hydrodeoxygenation Processes: Advances on Catalytic Transformations of Biomass-Derived Platform Chemicals into Hydrocarbon Fuels. *Bioresour. Technol.* **2015**, *178*, 108–118. [CrossRef]
20. Duan, D.; Chen, D.; Huang, L.; Zhang, Y.; Zhang, Y.; Wang, Q.; Xiao, G.; Zhang, W.; Lei, H.; Ruan, R. Activated Carbon from Lignocellulosic Biomass as Catalyst: A Review of the Applications in Fast Pyrolysis Process. *J. Anal. Appl. Pyrolysis* **2021**, *158*, 105246. [CrossRef]
21. Danquah, J.A.; Roberts, C.O.; Appiah, M. Elephant Grass (*Pennisetum Purpureum*): A Potential Source of Biomass for Power Generation in Ghana. *Curr. J. Appl. Sci. Technol.* **2018**, *30*, 1–12. [CrossRef]
22. Ohimain, E.I.; Kendabie, P.; Nwachukwu, R.E.S. Bioenergy Potentials of Elephant Grass, *Pennisetum Purpureum* Schumach. *Annu. Res. Rev. Biol.* **2014**, *4*, 2215–2227. [CrossRef]
23. Williams, C. Fertilizer Response of Napier Grass under Different Soil Conditions in Brunei. *Exp. Agric.* **1980**, *16*, 415–423. [CrossRef]
24. Reza, M.S.; Azad, A.K.; Bakar, M.S.A.; Karim, M.R.; Sharifpur, M.; Taweekun, J. Evaluation of Thermochemical Characteristics and Pyrolysis of Fish Processing Waste for Renewable Energy Feedstock. *Sustainability* **2022**, *14*, 1203. [CrossRef]
25. Cheng, D.; Ngo, H.H.; Guo, W.; Chang, S.W.; Nguyen, D.D.; Zhang, X.; Varjani, S.; Liu, Y. Feasibility Study on a New Pomelo Peel Derived Biochar for Tetracycline Antibiotics Removal in Swine Wastewater. *Sci. Total Environ.* **2020**, *720*, 137662. [CrossRef]
26. Xu, J.; Chen, L.; Qu, H.; Jiao, Y.; Xie, J.; Xing, G. Preparation and Characterization of Activated Carbon from Reedy Grass Leaves by Chemical Activation with H₃PO₄. *Appl. Surf. Sci.* **2014**, *320*, 674–680. [CrossRef]
27. Reza, M.S.; Hasan, A.B.M.K.; Ahmed, A.S.; Afroze, S.; Bakar, M.S.A.; Islam, S.N.; Azad, A.K. COVID-19 Prevention: Role of Activated Carbon. *J. Eng. Technol. Sci.* **2021**, *53*, 210404. [CrossRef]
28. Gaber, A.; Saif, H.; Ali, M.R.O. Sugarcane Bagasse Pyrolysis: Investigating the Effect of Process Parameters on the Product Yields. *Mater. Sci. Forum* **2020**, *1008*, 159–167. [CrossRef]
29. NIST Standard Reference Database 1A NIST/EPA/NIH Mass Spectral Library (NIST 08) and NIST Mass Spectral Search Program (Version 2.0f). Available online: <https://chemdata.nist.gov/mass-spc/ms-search/docs/Ver20Man.pdf> (accessed on 5 March 2023).
30. Reza, M.S.; Islam, S.N.; Afroze, S.; Bakar, M.S.A.; Taweekun, J.; Azad, A.K. Data on FTIR, TGA–DTG, DSC of Invasive *Pennisetum Purpureum* Grass. *Data Br.* **2020**, *30*, 105536. [CrossRef]
31. Suhas; Carrott, P.J.M.; Ribeiro Carrott, M.M.L. Lignin—From Natural Adsorbent to Activated Carbon: A Review. *Bioresour. Technol.* **2007**, *98*, 2301–2312. [CrossRef]
32. Ahmed, M.J. Preparation of Activated Carbons from Date (*Phoenix Dactylifera* L.) Palm Stones and Application for Wastewater Treatments: Review. *Process Saf. Environ. Prot.* **2016**, *102*, 168–182. [CrossRef]
33. Aslam, Z.; Anait, U.; Abbas, A.; Ihsanullah, I.; Irshad, U.; Mahmood, N. Adsorption of Carbon Dioxide onto Activated Carbon Prepared from Lawn Grass. *Biomass Convers. Biorefin.* **2020**, *12*, 3121–3131. [CrossRef]
34. Lü, L.; Lu, D.; Chen, L.; Luo, F. Removal of Cd(II) by Modified Lawn Grass Cellulose Adsorbent. *Desalination* **2010**, *259*, 120–130. [CrossRef]
35. Hernandez-Soriano, M.C.; Kerré, B.; Kopittke, P.M.; Horemans, B.; Smolders, E. Biochar Affects Carbon Composition and Stability in Soil: A Combined Spectroscopy-Microscopy Study. *Sci. Rep.* **2016**, *6*, 25127. [CrossRef]
36. Song, W.; Guo, M. Quality Variations of Poultry Litter Biochar Generated at Different Pyrolysis Temperatures. *J. Anal. Appl. Pyrolysis* **2012**, *94*, 138–145. [CrossRef]
37. Yang, H.; Yan, R.; Chen, H.; Lee, D.H.; Zheng, C. Characteristics of Hemicellulose, Cellulose and Lignin Pyrolysis. *Fuel* **2007**, *86*, 1781–1788. [CrossRef]
38. Popescu, C.; Popescu, M.; Singurel, G.; Vasile, C.; Argyropoulos, D.S.; Willfor, S. Spectral Characterization of Eucalyptus Wood. *Soc. Appl. Spectrosc.* **2018**, *61*, 1168–1177. [CrossRef]
39. Mopoung, S.; Moonsri, P.; Palas, W.; Khumpai, S. Characterization and Properties of Activated Carbon Prepared from Tamarind Seeds by KOH Activation for Fe(III) Adsorption from Aqueous Solution. *Sci. World J.* **2015**, *2015*, 415961. [CrossRef]
40. Özçimen, D.; Ersoy-Meriçboyu, A. Characterization of Biochar and Bio-Oil Samples Obtained from Carbonization of Various Biomass Materials. *Renew. Energy* **2010**, *35*, 1319–1324. [CrossRef]
41. Zhang, H.; Wang, Y.; Shao, S.; Xiao, R. Catalytic Conversion of Lignin Pyrolysis Model Compound- Guaiacol and Its Kinetic Model Including Coke Formation. *Sci. Rep.* **2016**, *6*, 37513. [CrossRef]
42. Ao, W.; Fu, J.; Mao, X.; Kang, Q.; Ran, C.; Liu, Y.; Zhang, H.; Gao, Z.; Li, J.; Liu, G.; et al. Microwave Assisted Preparation of Activated Carbon from Biomass: A Review. *Renew. Sustain. Energy Rev.* **2018**, *92*, 958–979. [CrossRef]
43. Abu Bakar, M. Catalytic Intermediate Pyrolysis of Brunei Rice Husk for Bio-Oil Production. Ph.D. Thesis, Aston University, Birmingham, UK, 2013.
44. Mamaeva, A.; Tahmasebi, A.; Tian, L.; Yu, J. Microwave-Assisted Catalytic Pyrolysis of Lignocellulosic Biomass for Production of Phenolic-Rich Bio-Oil. *Bioresour. Technol.* **2016**, *211*, 382–389. [CrossRef]
45. Zhang, Y.; Lei, H.; Yang, Z.; Duan, D.; Villota, E.; Ruan, R. From Glucose-Based Carbohydrates to Phenol-Rich Bio-Oils Integrated with Syngas Production via Catalytic Pyrolysis over an Activated Carbon Catalyst. *Green Chem.* **2018**, *20*, 3346–3358. [CrossRef]

46. Ratnasari, D.K.; Yang, W.; Jönsson, P.G. Catalytic Pyrolysis of Lignocellulosic Biomass: The Influence of the Catalyst Regeneration Sequence on the Composition of Upgraded Pyrolysis Oils over a H-ZSM-5/Al-MCM-41 Catalyst Mixture. *ACS Omega* **2020**, *5*, 28992–29001. [[CrossRef](#)] [[PubMed](#)]
47. Garcia-Perez, M.; Chaala, A.; Pakdel, H.; Kretschmer, D.; Roy, C. Characterization of Bio-Oils in Chemical Families. *Biomass Bioenergy* **2007**, *31*, 222–242. [[CrossRef](#)]
48. Ingram, L.; Mohan, D.; Bricka, M.; Steele, P.; Strobel, D.; Crocker, D.; Mitchell, B.; Mohammad, J.; Cantrell, K.; Pittman, C.U. Pyrolysis of Wood and Bark in an Auger Reactor: Physical Properties and Chemical Analysis of the Produced Bio-Oils. *Energy Fuels* **2008**, *22*, 614–625. [[CrossRef](#)]
49. Moens, L.; Black, S.K.; Myers, M.D.; Czernik, S. Study of the Neutralization and Stabilization of a Mixed Hardwood Bio-Oil. *Energy Fuels* **2009**, *23*, 2695–2699. [[CrossRef](#)]
50. Yorgun, S.; Yildiz, D. Slow Pyrolysis of Paulownia Wood: Effects of Pyrolysis Parameters on Product Yields and Bio-Oil Characterization. *J. Anal. Appl. Pyrolysis* **2015**, *114*, 68–78. [[CrossRef](#)]
51. Lv, G.; Wu, S. Analytical Pyrolysis Studies of Corn Stalk and Its Three Main Components by TG-MS and Py-GC/MS. *J. Anal. Appl. Pyrolysis* **2012**, *97*, 11–18. [[CrossRef](#)]
52. Lu, Q.; Zhang, Y.; Tang, Z.; Li, W.Z.; Zhu, X.F. Catalytic Upgrading of Biomass Fast Pyrolysis Vapors with Titania and Zirconia/titania Based Catalysts. *Fuel* **2010**, *89*, 2096–2103. [[CrossRef](#)]
53. Kim, T.-S.; Kim, J.-Y.; Kim, K.-H.; Lee, S.; Choi, D.; Choi, I.-G.; Choi, J.W. The Effect of Storage Duration on Bio-Oil Properties. *J. Anal. Appl. Pyrolysis* **2012**, *95*, 118–125. [[CrossRef](#)]
54. Williams, P.T.; Horne, P.A. Characterisation of Oils from the Fluidised Bed Pyrolysis of Biomass with Zeolite Catalyst Upgrading. *Biomass Bioenergy* **1994**, *7*, 223–236. [[CrossRef](#)]
55. Mullen, C.A.; Tarves, P.C.; Boateng, A.A. Role of Potassium Exchange in Catalytic Pyrolysis of Biomass over ZSM-5: Formation of Alkyl Phenols and Furans. *ACS Sustain. Chem. Eng.* **2017**, *5*, 2154–2162. [[CrossRef](#)]
56. Binder, J.B.; Raines, R.T. Simple Chemical Transformation of Lignocellulosic Biomass into Furans for Fuels and Chemicals. *J. Am. Chem. Soc.* **2009**, *131*, 1979–1985. [[CrossRef](#)] [[PubMed](#)]
57. Zhang, Q.; Chang, J.; Wang, T.; Xu, Y. Review of Biomass Pyrolysis Oil Properties and Upgrading Research. *Energy Convers. Manag.* **2007**, *48*, 87–92. [[CrossRef](#)]
58. Liu, W.J.; Li, W.W.; Jiang, H.; Yu, H.Q. Fates of Chemical Elements in Biomass during Its Pyrolysis. *Chem. Rev.* **2017**, *117*, 6367–6398. [[CrossRef](#)]
59. Prado, G.H.C.; Rao, Y.; De Klerk, A. Nitrogen Removal from Oil: A Review. *Energy Fuels* **2017**, *31*, 14–36. [[CrossRef](#)]
60. Iliopoulou, E.F.; Stefanidis, S.D.; Kalogiannis, K.G.; Delimitis, A.; Lappas, A.A.; Triantafyllidis, K.S. Catalytic Upgrading of Biomass Pyrolysis Vapors Using Transition Metal-Modified ZSM-5 Zeolite. *Appl. Catal. B Environ.* **2012**, *127*, 281–290. [[CrossRef](#)]
61. Stefanidis, S.D.; Kalogiannis, K.G.; Iliopoulou, E.F.; Michailof, C.M.; Pilavachi, P.A.; Lappas, A.A. A Study of Lignocellulosic Biomass Pyrolysis via the Pyrolysis of Cellulose, Hemicellulose and Lignin. *J. Anal. Appl. Pyrolysis* **2014**, *105*, 143–150. [[CrossRef](#)]
62. Sadare, O.O.; Obazu, F.; Daramola, M.O. Biodesulfurization of Petroleum Distillates—Current Status, Opportunities and Future Challenges. *Environments* **2017**, *4*, 85. [[CrossRef](#)]
63. Thomas, V.M.; Bedford, J.A.; Cicerone, R.J. Bromine Emissions from Leaded Gasoline. *Geophys. Res. Lett.* **1997**, *24*, 1371–1374. [[CrossRef](#)]
64. Duan, D.; Zhang, Y.; Wang, Y.; Lei, H.; Wang, Q.; Ruan, R. Production of Renewable Jet Fuel and Gasoline Range Hydrocarbons from Catalytic Pyrolysis of Soapstock over Corn Cob-Derived Activated Carbons. *Energy* **2020**, *209*, 118454. [[CrossRef](#)]
65. Shan Ahamed, T.; Anto, S.; Mathimani, T.; Brindhadevi, K.; Pugazhendhi, A. Upgrading of Bio-Oil from Thermochemical Conversion of Various Biomass—Mechanism, Challenges and Opportunities. *Fuel* **2021**, *287*, 119329. [[CrossRef](#)]
66. Upreti, G.K.; Awad, S.; Burnens, G.; Kassargy, C.; Tazerout, M. Experimental Investigation on the Reduction of Catalyst Costs in the Polyethylene Pyrolysis Process. *IOP Conf. Ser. Earth Environ. Sci.* **2018**, *105*, 12122. [[CrossRef](#)]
67. Huo, E.; Duan, D.; Lei, H.; Liu, C.; Zhang, Y.; Wu, J.; Zhao, Y.; Huang, Z.; Qian, M.; Zhang, Q.; et al. Phenols Production from Douglas Fir Catalytic Pyrolysis with MgO and Biomass-Derived Activated Carbon Catalysts. *Energy* **2020**, *199*, 117459. [[CrossRef](#)]
68. Tan, S.; Zhang, Z.; Sun, J.; Wang, Q. Recent Progress of Catalytic Pyrolysis of Biomass by HZSM-5. *Cuihua Xuebao/Chin. J. Catal.* **2013**, *34*, 641–650. [[CrossRef](#)]
69. Vitolo, S.; Bresci, B.; Seggiani, M.; Gallo, M.G. Catalytic Upgrading of Pyrolytic Oils over HZSM-5 Zeolite: Behaviour of the Catalyst When Used in Repeated Upgrading-Regenerating Cycles. *Fuel* **2001**, *80*, 17–26. [[CrossRef](#)]
70. Bu, Q.; Lei, H.; Wang, L.; Wei, Y.; Zhu, L.; Liu, Y.; Liang, J.; Tang, J. Renewable Phenols Production by Catalytic Microwave Pyrolysis of Douglas Fir Sawdust Pellets with Activated Carbon Catalysts. *Bioresour. Technol.* **2013**, *142*, 546–552. [[CrossRef](#)]
71. Yang, C.; Jia, L.; Chen, C.; Liu, G.; Fang, W. Bio-Oil from Hydro-Liquefaction of Dunaliella Salina over Ni/REHY Catalyst. *Bioresour. Technol.* **2011**, *102*, 4580–4584. [[CrossRef](#)]
72. Obeid, F.; Chu Van, T.; Brown, R.; Rainey, T. Nitrogen and Sulphur in Algal Biocrude: A Review of the HTL Process, Upgrading, Engine Performance and Emissions. *Energy Convers. Manag.* **2019**, *181*, 105–119. [[CrossRef](#)]
73. Cigno, E.; Magagnoli, C.; Pierce, M.S.; Iglesias, P. Lubricating Ability of Two Phosphonium-Based Ionic Liquids as Additives of a Bio-Oil for Use in Wind Turbines Gearboxes. *Wear* **2017**, *376–377*, 756–765. [[CrossRef](#)]

74. Baloch, H.A.; Nizamuddin, S.; Siddiqui, M.T.H.; Riaz, S.; Konstas, K.; Mubarak, N.M.; Srinivasan, M.P.; Griffin, G.J. Catalytic Upgradation of Bio-Oil over Metal Supported Activated Carbon Catalysts in Sub-Supercritical Ethanol. *J. Environ. Chem. Eng.* **2021**, *9*, 105059. [[CrossRef](#)]
75. Pham, T.N.; Sooknoi, T.; Crossley, S.P.; Resasco, D.E. Ketonization of Carboxylic Acids: Mechanisms, Catalysts, and Implications for Biomass Conversion. *ACS Catal.* **2013**, *3*, 2456–2473. [[CrossRef](#)]
76. Dinh Ngo, S.; Tuong Vi Tran, T.; Kongparakul, S.; Reubroycharoen, P.; Kidkhuntod, P.; Chanlek, N.; Wang, J.; Guan, G.; Samart, C. Catalytic Pyrolysis of Napier Grass with Nickel-Copper Core-Shell Bi-Functional Catalyst. *J. Anal. Appl. Pyrolysis* **2020**, *145*, 104745. [[CrossRef](#)]
77. Mohamed, B.A.; Ellis, N.; Kim, C.S.; Bi, X. Synergistic Effects of Catalyst Mixtures on Biomass Catalytic Pyrolysis. *Front. Bioeng. Biotechnol.* **2020**, *8*, 1391. [[CrossRef](#)] [[PubMed](#)]
78. Weber, M.; Weber, M.; Weber, V. Phenol. In *Ullmann's Encyclopedia of Industrial Chemistry*; Wiley: Weinheim, Germany, 2020; pp. 1–20.
79. Fiege, H. Cresols and Xylenols. In *Ullmann's Encyclopedia of Industrial Chemistry*; Wiley-VCH Verlag GmbH & Co. KGaA: Weinheim, Germany, 2000.
80. Fiege, H.; Voges, H.-W.; Hamamoto, T.; Umemura, S.; Iwata, T.; Miki, H.; Fujita, Y.; Buysch, H.-J.; Garbe, D.; Paulus, W. Phenol Derivatives. In *Ullmann's Encyclopedia of Industrial Chemistry*; Wiley-VCH Verlag GmbH & Co. KGaA: Weinheim, Germany, 2000.
81. Müller, H. Tetrahydrofuran. In *Ullmann's Encyclopedia of Industrial Chemistry*; Wiley-VCH Verlag GmbH & Co. KGaA: Weinheim, Germany, 2000.
82. Peng, J.; Chen, P.; Lou, H.; Zheng, X. Catalytic Upgrading of Bio-Oil by HZSM-5 in Sub- and Super-Critical Ethanol. *Bioresour. Technol.* **2009**, *100*, 3415–3418. [[CrossRef](#)]

Disclaimer/Publisher's Note: The statements, opinions and data contained in all publications are solely those of the individual author(s) and contributor(s) and not of MDPI and/or the editor(s). MDPI and/or the editor(s) disclaim responsibility for any injury to people or property resulting from any ideas, methods, instructions or products referred to in the content.